HHS Public Access

Author manuscript

Toxicol Appl Pharmacol. Author manuscript; available in PMC 2017 December 30.

Published in final edited form as:

Toxicol Appl Pharmacol. 2017 September 15; 331: 6–17. doi:10.1016/j.taap.2017.03.017.

Transient and permanent changes in DNA methylation patterns in inorganic arsenic-mediated epithelial-to-mesenchymal transition

Meredith Eckstein, **Matthew Rea**, and **Yvonne N. Fondufe-Mittendorf***

Department of Molecular and Cellular Biochemistry, University of Kentucky, Lexington, KY 40536, USA

Abstract

Chronic low dose inorganic arsenic exposure causes cells to take on an epithelial-to-mesenchymal phenotype, which is a crucial process in carcinogenesis. Inorganic arsenic is not a mutagen and thus epigenetic alterations have been implicated in this process. Indeed, during the epithelial-to-mesenchymal transition, morphologic changes to cells correlate with changes in chromatin structure and gene expression, ultimately driving this process. However, studies on the effects of inorganic arsenic exposure/withdrawal on the epithelial-to-mesenchymal transition and the impact of epigenetic alterations in this process are limited. In this study we used high-resolution microarray analysis to measure the changes in DNA methylation in cells undergoing inorganic arsenic-induced epithelial-to-mesenchymal transition, and on the reversal of this process, after removal of the inorganic arsenic exposure. We found that cells exposed to chronic, low-dose inorganic arsenic exposure showed 30,530 sites were differentially methylated, and with inorganic arsenic withdrawal several differential methylated sites were reversed, albeit not completely. Furthermore, these changes in DNA methylation mainly correlated with changes in gene expression at most sites tested but not at all. This study suggests that DNA methylation changes on gene expression are not clear-cut and provide a platform to begin to uncover the relationship between DNA methylation and gene expression, specifically within the context of inorganic arsenic treatment.

Keywords

Inorganic arsenic; DNA methylation; Infinium MethylationEPIC BeadChip; EMT; Epigenetics

*Corresponding author at: 741 S. Limestone, BBSRB 273, Lexington, KY 40536, USA. y.fondufe-mittendorf@uky.edu (Y.N. Fondufe-Mittendorf).

Conflict of interest statement

The authors state no conflicts of interest pertaining to this work.

Transparency document

The Transparency document associated with this article can be found in online version.

Appendix A. Supplementary data

Supplementary data to this article can be found online at http://dx.doi.org/10.1016/j.taap.2017.03.017.

1. Introduction

Environmental inorganic arsenic (iAs) exposure through contaminated water consumption represents a major public health concern (IARC, 2004; Tapio and Grosche, 2006; Salnikow and Zhitkovich, 2008; States et al., 2009; Cheng et al., 2012) and has been linked to cardiovascular diseases (States et al., 2009; Garcia-Esquinas et al., 2013), diabetes (Drobná et al., 2013), and a variety of cancers including lung (Hopenhayn-Rich et al., 1998), colorectal (Johnson et al., 2011), kidney (Hopenhayn-Rich et al., 1998), liver (Hopenhayn-Rich et al., 1998; Chen et al., 2004) and skin cancers (Tseng et al., 1968; Rossman et al., 2001). Inorganic arsenic is not a direct mutagen, rather it acts through other mechanisms to induce cellular transformation and epithelial-to-mesenchymal transition (EMT) (Rossman, 2003; Klein et al., 2007). Several mechanisms have been proposed to describe how iAs-induced toxicity promotes carcinogenesis; these include the induction of oxidative stress (Huang et al., 1999; Harris and Shi, 2003; Huang et al., 2004), inhibition of DNA repair, and chromosomal aberrations (Collins et al., 1995; Klein et al., 2007). In addition to these mechanisms, recent findings indicate that epigenetic factors, such as DNA methylation, play a central role in aberrant gene expression resulting from iAs exposure (Li et al., 2002; Li et al., 2008; Zhou et al., 2008, 2011).

DNA methylation, the most stable epigenetic mark, is a key factor in regulating gene expression (Robertson, 2005; Suzuki and Bird, 2008). This mark is catalyzed by DNA methyltransferases (DNMTs); DNMT1 is responsible for the maintenance methylation while DNMT3a and DNMT3b perform *de novo* methylation (Bestor, 2000; Goll and Bestor, 2005). DNA methyltransferases facilitate this modification by the transfer of a methyl group from *S*-adenosyl methionine (SAM) to the 5′ carbon of cytosine residues (Bestor, 2000). This modification normally occurs in regions/contexts of high CpG density, known as CpG islands (CGIs). However, DNA methylation can also occur in non-CGI contexts. CGIs are typically concentrated at promoter regions but can be found in other regions (Bird, 2002) and methylation controls gene expression differently depending on its location. The presence of 5-methylcytosine at promoters is usually associated with transcriptional repression (Bird, 2002). Conversely, absence of this mark, along with the presence of the appropriate transcription factors, promotes gene expression. However, within gene bodies and at intergenic regions, the effects of methylation are less definitive; therefore, studies are in process to elucidate the dynamic effects of DNA methylation in those contexts. Since methylation affects transcription factor binding ability (Perini et al., 2005), it is possible that DNA methylation functions prominently in cell and tissue identity and functionality.

Several mechanisms have been proposed to describe how iAs affects the DNA methylation profile in cells. The first involves the metabolism of inorganic arsenic. During iAs metabolism, arsenic methyltransferase (AS3MT) transfers a methyl group to arsenite, using SAM as a donor (Miao et al., 2015); this process could lead to a depletion of SAM, which is needed for a variety of other cellular processes. A second mechanism involves changes in the expression of DNMTs in response to chronic exposure to iAs. In trying to understand why DNMTs would be targeted, we found that the transcriptional repressor CTCF is targeted by iAs treatment, causing changes in CTCF occupancy at DNMT promoters (Cui et

al., 2006; Li et al., 2015a; Rea et al., 2017). Such disruption in the DNMT expression would effect changes in DNA methylation patterns.

Several studies that focus on profiling of the global changes in DNA methylation levels have been carried out in cells exposed to iAs; however, these studies have used low-resolution genome profiling techniques to investigate methylation patterns (Koestler et al., 2013). Clearly missing is an analysis of DNA methylation patterns at gene regulatory regions such as CpG islands, promoters, and enhancers. Recently, we carried out the first comprehensive study of DNA methylation changes with single-nucleotide resolution for cells chronically exposed to low doses of arsenic (Rea et al., 2017). In the present study, we extend our findings to determine changes in iAs-induced DNA methylation patterns in cells with chronic low-dose iAs exposure, as well as in cells that undergo a reversal of this treatment. Our studies include the analysis of DNA methylation profiles and correlations of gene expression changes in the cells, combining unbiased whole-genome and candidate gene approaches.

In this study, we aim to determine the effect of iAs on both permanent and reversible changes in DNA methylation and gene expression that drive EMT. Our lab previously showed that removal of iAs resulted in a reversal of some gene expression patterns (Riedmann et al., 2015; Rea et al., 2016). We reasoned that since epigenetic marks are reversible, some methylation patterns would revert to the nontreated condition when iAs is removed, thereby reversing some gene expression patterns, while others would remain stable. We therefore investigated the adaptive changes after reversal of the exposure.

2. Materials and methods

2.1. HeLa cell growth conditions and treatment

HeLa cells were grown using Dulbecco's modified Eagle medium (Sigma-Aldrich, St. Louis, MO) supplemented with 10% fetal bovine serum (Sigma-Aldrich), 1% MEM nonessential amino acids (Sigma-Aldrich), and 1% penicillin-streptomycin (Sigma-Aldrich). Cells were grown in a humidified chamber at 37 °C and 5% CO_2 until they reached 80% confluency. For iAs exposure, cells were treated with 0.5 μM sodium arsenite (Sigma-Aldrich) for approximately 45 days. Time matched controls were treated with water (nontreated or NT cells). Reverse treated cells were treated with 0.5 μM sodium arsenite until day 36, at which point they were treated with water instead of sodium arsenite. Reverse treated cells were harvested 10 days after treatment reversal (day 46).

2.2. Western blot analysis

Whole cell protein was extracted from 5×10^6 HeLa cells. Cells were intermittently sonicated with 12 cycles of 30 s bursts/30 s rest (Diagenode Bioruptor 300) and centrifuged at 13000 rpm at 4 °C for 15 min to pellet cell debris. Protein concentration was measured using a BCA kit (Thermo Fisher) and 30 μg of total protein were run on a 10% or 15% SDS-PAGE gel at 120 V until loading dye reached the bottom of the gel. Proteins were transferred to polyvinylidene fluoride membranes (PVDF) at 65 V for 90 min on ice. 5% milk + phosphate buffered saline with Tween (PBST) was used to block non-specific binding to the

membranes. Membranes were incubated with primary antibodies (Cell Signaling Technologies, Danvers, MA #9782, EMT Antibody Sampler Kit) (in 0.5% milk + PBST) overnight at 4 °C and then with secondary antibody (α-rabbit or α-mouse) the next day. Proteins were visualized with ECF (GE-Typhoon FLA9500) as outlined by the manufacturer.

2.3. Quantification of the 5-methylcytosine level in DNA

Genomic DNA was isolated from the cells and total 5-methylcytosine (5-mC) was determined using the 5-mC DNA ELISA kit (Zymo Research Corp., Irvine, CA, USA) per the manufacturer's instruction. Briefly, DNA is denatured and then treated with an anti-5-methylcytosine monoclonal antibody that is both sensitive and specific for 5-mC. A secondary antibody containing horseradish peroxidase is then used to detect 5mC. Values are expressed as a percent 5-mC in a DNA sample calculated through a standard curve generated with specially designed controls that are included in the kit. Each ELISA was performed in triplicate and students *t*-test ($p < 0.05$) determined statistical significance.

2.4. Infinium MethylationEPIC BeadChip - methylation array analysis

2.4.1. Sample preparation for the chip—Genomic DNA from nontreated, treated, and reverse treated cells was extracted using the Qiagen DNeasy Blood and Tissue kit; samples were initially bisulfite converted using the Zymo EZ-96DNA Methylation Kit (Catalog #D5004) Deep-Well Format. DNA was treated with sodium bisulfite causing unmethylated cytosines to convert to uracil while keeping methylated cytosines unchanged. Then 4 μl (equivalent to 750 ng DNA) of the bisulfite- converted DNA was used as input for the Illumina Infinium HD Methylation Array. During this process, the bisulfite converted DNA samples were denatured, neutralized, and prepared for amplification. The amplified DNA was enzymatically fragmented and precipitated. The resuspended DNA samples were then dispensed onto Illumina's Infinium MethylationEPIC BeadChip, where they underwent a series of washing, extension, and staining procedures. The BeadChips are then coated for protection and scanned on the Illumina HiScanSQ. Once scanning was completed, the data were uploaded into GenomeStudio for preliminary and quality control analysis.

2.4.2. Data analyses—Target success rates were determined and the detection p-value was calculated as 1-p from the background model characterizing the chance that the target sequence was distinguishable from the negative control. Poor performing targets were defined as having $p > 0.05$ and were discarded. Sample replicates were checked for an r^2 value >0.99. For statistical analysis, beta values were calculated. The methylation levels of CpGs were described as beta values (0 to 1) representing the calculated level of methylation (0% to 100%). We had two technical and two biological replicates processed by chip technique. The Pearson correlation coefficients (PCCs) were >0.99 for all the replicates, confirming a good level of reproducibility for the chip process and indicating that the observed differential methylation between the cells (treatments) represented true biological differences. Functional normalization was performed using home scripts ‘Minfi preprocessFunNorm’ which does the background normalization. Additionally, the dye correction was performed using noob. All CpG sites with a detection value > 0.05, CpG sites with SNPs, as well as probes predicted to hybridize to more than one genomic location

(identified by McCartney et al. in Genomics Data, 2016) were removed. Experiments were done in duplicate and a high concordance was observed within each group.

2.5. qRT-PCR

RNA was isolated from 5×10^6 HeLa cells using an RNeasy Mini Kit (Qiagen). A reverse transcriptase reaction was set up containing iScript Reverse Transcriptase (Bio-Rad #1708891) and 1 μg of RNA, producing cDNA. Each qRT-PCR reaction contained 25 ng of cDNA and followed the following reaction protocol: 1) 94 °C for 5 min; 2) 94 °C for 30 s; 3) 53– 65 °C (dependent on primer pair; Supplemental Table 1) for 30 s; 4) 72 °C for 45 s; 5) repeat 2–4 for 40 cycles; 6) 72 °C for 10 min. Primers for the housekeeping gene, GAPDH, were made using PrimerBank. qRT-PCR data was analyzed by the 2^{-ddCt} method and student *t*-tests were performed to determine statistical significance.

3. Results

3.1. Cellular transformation and EMT

To determine the effect of iAs on the epithelial-to-mesenchymal transition (EMT), we used the common cervical cancer cell line, HeLa, which has been used extensively to study cell signaling and EMT (Deng et al., 2015; Li et al., 2015b; Riedmann et al., 2015). Interestingly, though carcinogenic, HeLa cells can still undergo EMT (Xiao et al., 2013), and specifically, iAs-induced EMT (Riedmann et al., 2015; Rea et al., 2016). In our experimental design (Fig. 1A), HeLa media was replenished with 0.5 μM sodium arsenite every three to four days for 45 days to allow cells to undergo iAs-mediated EMT (iAsT). This low-dose treatment simulates chronically exposed, environmentally relevant iAs levels that many people in mining regions experience (Nordstrom, 2002; IARC, 2004; NTP, 2014). We confirm our previous results showing that chronic low-dose treatment of cells with iAs resulted in epithelial-to-mesenchymal transition in HeLa cells (Riedmann et al., 2015; Rea et al., 2016; Rea et al., 2017). In addition, after continuous exposure, iAs was removed from some cultures and those cells were grown in media without iAs for 10 more days. We called this period of treatment without iAs “inorganic arsenic exposure reversal” (iAs-rev) and its purpose is to simulate situations where people are removed from chronic iAs exposure (Fig. 1A).

In previous studies, we observed EMT through cell morphology as well as through qRT-PCR and western blot analyses of EMT markers (Riedmann et al., 2015; Rea et al., 2016, 2017). Morphologically, we observed that NT cells maintained an epithelial phenotype in which cells were round and small. Upon iAs treatment, cells developed a more mesenchymal phenotype, being elongated and spindle-shaped, suggestive of EMT (Riedmann et al., 2015; Rea et al., 2016). Through qRT-PCR and western blot analyses, we observed changes to cellular markers characteristic of cells undergoing the EMT process. Cell adhesion markers, such as β-catenin, Claudin-1, Claudin-3, and ZO-1, are expected to decrease in expression while transcription factors that promote a mesenchymal phenotype, such as Snail, Slug, and Vimentin, are expected to increase in expression (Riedmann et al., 2015; Rea et al., 2016). Additionally, upon reversal of treatment, we found that some EMT markers exhibited a moderate reversal in expression and protein levels (β-catenin, Slug, and Snail) while others

did not revert (Claudin-3 and Vimentin) (Rea et al., 2016). To validate that EMT is occurring in our current studies, we analyzed protein expression changes for EMT markers using western blot analysis and the changes in protein levels indicate that the cells indeed had undergone EMT (Fig. 1B). We found that Claudin-1 decreased in protein levels upon treatment and that Slug, N-cadherin, and Snail increased upon treatment. After reversal of treatment, some markers exhibited a moderate reversal such as Slug and N-cadherin, indicating that there was some reversal of the EMT conditions albeit not completely. Conversely, Claudin-1 and Snail did not revert back towards nontreated levels, which we also saw in previous studies (Fig. 1B). These results corroborate our previous data, indicating that cells treated with low doses of inorganic arsenic undergo EMT and that this transition is partially reversed when inorganic arsenic is removed.

3.2. Global DNA methylation level

After demonstrating that HeLa cells undergo EMT in response to iAs treatment and partial reversal with iAs withdrawal, we next identified the DNA methylation changes present in iAsT and iAs-rev cells. We first determined the levels of global DNA methylation in these samples using the Zymo 5-mC DNA ELISA assay. We found significantly higher DNA methylation levels in iAsT cells compared to NT cells (Fig. 2). In line with our reversal of EMT markers, we observed a reduction in global DNA methylation levels in iAs-rev cells compared to iAsT cells, and the amount of DNA methylation more closely resembled those in NT cells (Fig. 2). We interpret these data as indicating that global DNA methylation is reprogrammed in these cells and may correlate with changes in gene expression patterns.

3.3. Quantification of DNA methylation at specific sites

Since the 5MC DNA ELISA assay is a low-resolution technique that measures DNA methylation levels and only surveys a small sample of CpG sites, the Infinium MethylationEPIC BeadChip Array was used to further interrogate the differential methylation patterns globally, and at specific genes targeted in iAs-mediated EMT and reversal. This array has 853,307 CpG (850 K) sites, providing the ability to interrogate DNA methylation changes not only at promoters and gene bodies, but also at unexplored regions such as enhancers. Indeed, incorporated into this Chip are 333,265 CpG sites, including enhancer regions identified by the ENCODE (The, 2012; Siggens and Ekwall, 2014) and FANTOM5 (Lizio et al., 2015) projects. Thus, this is a valuable tool to decipher how DNA methylation changes in unexplored territories, such as enhancer sequences, contribute to arsenic-mediated diseases.

3.4. Global methylation changes

To identify possible targets for iAs-mediated DNA methylation reprogramming, we conducted methylation profiling of the NT, iAsT, and iAs-rev cells. We filtered DNA methylation data according to the following criteria: methylation changes should be more than two-fold and should have a p-value < 0.05 (Supplemental Figs. 1 and 2). Of the 853,307 CpG sites, significant differences in DNA methylation were observed at 30,530 CpG sites in iAsT when compared to NT, of which 67% (20,314 CpG) were hypermethylated and 33% (10,216 CpGs) were hypomethylated (Fig. 3). Upon reversal of arsenic treatment, some of the methylated sites did not revert to normal methylation in NT

conditions. A total of 53% of the DMRs still differed from NT cells; 77% of these CpGs (10,996 CpGs) were hypermethylated, while 23% (3,3339 CpGs) were hypomethylated (Fig. 3). We then compared the DMRs in iAsT cells and iAs-rev cells. We observed that ~40,000 sites had reverted towards the wildtype status - 20,997 hypomethylated and 20,589 hypermethylated (Fig. 3). We hypothesize that although many DMRs revert to NT conditions, some were not reversed completely and so were still measured as DMRs by our analysis. While these global measurements are useful, they do not show differential methylation at specific gene regulatory regions.

3.5. iAs mediated DNA methylation changes in CGIs and non-island regions

Methylation is often concentrated at CGIs but can also be found in the regions surrounding CGIs (Fig. 4A). According to Illumina, a CGI is defined as a region in which there is GC content >50% in at least a 200 base pair region. Comparative analysis of the methylation patterns in CGIs, shores, shelves and open seas revealed significant differences in methylation patterns across NT, iAsT, and iAs-rev cells in certain CGI-related regions. The shelves (in blue), across all of the comparisons, only exhibited 2–3% hypo- or hypermethylation changes, indicating that DNA methylation of these specific regions may not play a prominent role in iAs-mediated EMT (Fig. 4B–D, all pie charts). For the shores (in purple), a slight decrease in hypomethylation was observed when comparing iAs-rev v. NT and iAsT v. NT (Fig. 4B and C, top pie charts). The most prominent changes in hypomethylation were observed within the CGIs (in orange) and open sea regions (in green). There was an increase in hypomethylation (15% to 25%) at CGIs upon reversal (Fig. 4B and C, top pie charts). On the other hand, in the open sea regions, the amount of hypomethylation was reduced upon reversal (55% to 49%) (Fig. 4B and C, top pie charts). This shift in the ratio of CGI to open sea hypomethylation could suggest that hypomethylation changes at the CGIs are more permanent while hypomethylation changes at the open seas are more transient and more prone to reversal when iAs treatment is removed.

In the shores (in purple), a slight increase in hypermethylation was observed when comparing iAs-rev v. NT and iAsT v. NT, which compensates for the slight decrease in hypomethylation, noted above (Fig. 4B and C, bottom pie charts). This shift in differential methylation at the shores was confirmed by the presence of more hypermethylation than hypomethylation in the iAs-rev v. iAsT comparison in Fig. 4D. This finding could suggest that the changes in the hypomethylated loci are more transient, or that the hypermethylation previously observed in treated cells is more permanent. At the CGIs, there is an increase in hypermethylation (11% to 14%) upon arsenic withdrawal, similar to the increase in hypomethylation in that region (Fig. 4B and C, bottom pie charts). For iAs-rev v. iAsT, the CpG islands exhibited 12% hypomethylation and 13% hypermethylation (Fig. 4D). In the open sea regions, the amount of hypermethylation was reduced from 66% to 61% upon reversal (Fig. 4B and C, bottom pie charts). Both hypo- and hypermethylation were reduced to a similar extent in the open seas after arsenic treatment was removed. When comparing iAs-rev to iAsT, the open sea represented 64% of the hypomethylated regions and 58% of the hypermethylated regions (Fig. 4D). The decrease in hypermethylation at the open seas and the increase in hypermethylation at CGIs after iAs withdrawal (which was also seen

with hypomethylation) could indicate that differential methylation in the open seas is not as permanent as differential methylation in the CGIs.

3.6. iAs-mediated DNA methylation changes in genes and gene regulatory regions

There are several regulatory regions within a gene that modulate gene expression and repression (Fig. 5A). We asked if there were any transient and/or permanent iAs-mediated methylation changes within these regions. We compared the methylation profiles across different regions of genes – 5′ and 3′UTRs (orange and gray respectively), gene body (purple), first exon (green), and regions 200 and 1500 base pairs (bp) upstream to the transcription start sites (TSS200 blue and TSS1500 red). When compared to NT cells, differential hypomethylation in iAsT cells is as follows – 25% at TSS1500, 11% at TSS200, 15% at 5′UTR, 6% at first exon, 41% within the gene bodies and 2% within the 3′UTR (Fig. 5B, left bar). In all regions analyzed, there is a similar amount of hypo- and hypermethylation changes, except at the gene body and TSS1500, where we observed 41% hypomethylation to 49% hypermethylation and 25% hypomethylation to 19% hypermethylation. (Fig. 5B). We next asked if these methylation changes can be reversed by comparing DNA methylation patterns in NT cells and iAs-rev cells. Focusing mainly on the regions that were strongly differentially methylated, we first observed a 30% hypomethylation and a 45% hypermethylation change within the gene body (Fig. 5C). This seems to indicate a reversal of methylation patterns when considering the changes seen in iAsT cells in the gene body region. Surprisingly, we also observed a dramatic change in methylation at the first exon – 22% hypomethylation and 6% hypermethylation (Fig. 5C). However, our understanding of the implication of this shift in hypomethylation towards the first exon at the moment is not clear. Furthermore, the TSS1500, which exhibited 25% hypomethylation and 19% hypermethylation in iAsT cells compared to NT cells (Fig. 5B), also exhibited differential methylation in the reverse treated cells (Fig. 5C). In reversed conditions, compared to NT cells, the differential methylation pattern is 18% hypomethylation and 20% hypermethylation, which is the opposite of what was observed in iAsT cells, indicating that reversal of methylation patterns may be occurring upon removal of iAs treatment. In most cases, we observed some reversal in DNA methylation though it was not complete. To test directly if this is true, we compared methylation patterns in iAsT v. iAs-rev cells. Here too, we still observed differential methylation at the sites tested. The gene body had 52% hypomethylation and 48% hypermethylation (Fig. 5D). The TSS1500 exhibited 20% hypomethylation and 24% hypermethylation (Fig. 5D). These findings verify that reversal of iAs treatment reversed DNA methylation patterns in gene regulatory regions, albeit not completely.

In order to better understand the DNA methylation changes occurring in genic regions, we performed Venn diagram comparisons of the differentially methylated genes. To begin, we compared those genes that are differentially methylated after iAs treatment (iAsT v. NT) with those that are differentially methylated after reversal of treatment (iAs-rev v. NT). The overlapping genes, of which there are 3582, are genes that had more permanent changes in methylation (Supplemental Fig. 3A); our reasoning being that these differential methylation patterns are present in both iAsT and iAs-rev cells.

Next, we identified those genes whose methylation patterns reversed after removal of iAs by comparing genes that were differentially methylated after treatment (iAsT v. NT) to those that are differentially methylated between iAs-rev and iAsT cells. This comparison resulted in 6825 overlapping genes (Supplemental Fig. 3B). We consider these genes as those with methylation patterns that had reversed to normal conditions because the iAs methylation state is similar to NT but different from iAsT cells. This is further confirmed by looking at the overlap of genes that were hypomethylated in the iAs-T cells and those that were hypermethylated in the iAs-rev. Comparing these groups showed that about 82% of hypomethylated genes in iAsT showed hypermethylation in the iAs-rev (3472 genes of 4236 total genes), while 71% of genes that were hypermethylated in iAsT showed hypomethylation in iAs-rev cells (4103 genes of 5774 total genes) (Supplemental Fig. 4).

Finally, we compared genes that were differentially methylated in iAs-rev cells to those that were differentially methylated between iAs-rev and iAsT cells. There were 4490 overlapping genes and we interpret these genes as those that are in transition between the NT and iAsT methylation state since their methylation state did not remain permanently changed but also did not completely revert to normal levels (Supplemental Fig. 3C).

3.7. iAs mediated DNA methylation changes at promoter associated regions

Promoter methylation is normally associated with gene repression. Thus to gain insight into the function of iAs-mediated reprogramming of DNA methylation patterns, we next focused our analyses of DNA methylation changes at promoter regions. Comparing iAsT to NT cells, we observed a near 50% hypomethylation in promoter-associated regions, of which 3.71% hypomethylation was associated with cell type specific promoter regions (Fig. 6A, top pie chart). This result is reasonable considering we are using the same cell type throughout this study. We next investigated if hypomethylation changes in promoter associated regions persisted after reversal of treatment. It seems that in iAs-rev cells (iAs-rev v. NT), there was little change – 48.58% to 49.03%, in promoter-associated hypomethylation in iAsT cells compared to iAs-rev cells (Fig. 6A and B, top pie charts). This may suggest that hypomethylation in promoter associated regions is stable and permanent and does not revert back to normal conditions upon reversal of iAs treatment.

We next analyzed hypermethylation at promoters. In iAsT cells, there was 38% hypermethylation in promoter-associated regions with 3.24% hypermethylation associated with cell type specific promoter regions when compared to NT cells (Fig. 6A, bottom pie chart). Interestingly, after withdrawal of iAs treatment (iAs-rev v. NT), there was a large increase in hypermethylation at promoter-associated regions (38.16% to 60.66%) (Fig. 6A and B, bottom pie charts). This was also accompanied by a decrease in hypermethylation in unclassified regions (25.68% to 19.8%) and unclassified cell type specific regions (30.83% to 14.78) (Fig. 6A and B, bottom pie charts). This shift in ratio could suggest that hypermethylation in promoter-associated regions is more permanent while hypermethylation in unclassified regions is more transient and able to revert back to normal levels after iAs withdrawal. The stark increase in hypermethylation at promoter-associated regions is validated by a higher ratio of hypermethylation than hypomethylation in that region in the iAs-rev v. iAsT comparison (Fig. 6C). While investigating DNA methylation changes within

specific gene regions is advantageous for understanding their function, our understanding of DNA methylation in non-promoter regions is still in its infancy. In this study, we have focused our attention to promoter and gene body methylation at specific genes and the correlation of their methylation status to gene expression levels.

3.8. Coupling of differential methylation and differential gene expression at specific loci

Next we asked whether these differential methylation patterns affect gene expression at the transcript level. DNA methylation present at the promoters of genes is typically associated with gene repression, and demethylation leads to gene expression (Bird, 2002; Perini et al., 2005). On the other hand, the function of DNA methylation in gene body regions is not as definitive. It seems that methylation in the gene body functions in a manner opposite to that in the promoter region (Jjingo et al., 2012; Yang et al., 2014). In gene bodies, hypomethylation correlates with gene repression while hypermethylation correlates with gene expression (Yang et al., 2014). Additionally, DNA methylation in the gene body has been linked to regulation of alternative splicing so the full breadth of its function is still limited (Maunakea et al., 2013; Lev Maor et al., 2015; Yearim et al., 2015). To examine the impact of DNA methylation changes on gene expression in our experimental conditions, RNA was extracted from NT, iAsT and iAs-rev cells. This RNA was converted to cDNA and used for quantitative real time PCR analysis (qRT-PCR). For this analysis, we chose genes that showed significant differential methylation (Fig. 3) at the promoter region or within the gene body and that could potentially be implicated in EMT.

The first gene examined was *CORO1B*, which is important in cell motility regulation (Williams et al., 2012), and has hypomethylation at the promoter region (Table 1). qRT-PCR analysis at the transcript level of this gene showed an increase in gene expression in iAsT cells (Fig. 7A), correlating with the observed hypomethylation at the promoter region of this gene (Table 1). The level of gene expression remained high even after iAs was removed (iAs-rev cells), indicating that this change is more permanent. Interestingly, we were not able to identify any significant change in DNA methylation at the promoter of this gene in iAs-rev cells, possibly due to the cutoff stringency applied in the differential methylation analysis. The second gene we tested was *PPME1*, which plays a role in malignant glioma progression (Puustinen et al., 2009). qRT-PCR analysis showed no increase in gene expression in iAsT cells, though our genome-wide methylation data indicated this region as being hypermethylated (Table 1). This could possibly be explained by the fact that not all CpGs regulate gene expression. On the other hand, in iAs-rev cells, a significant increase in gene expression was observed (Fig. 7A), We also investigated the *PPM1L gene*, which is known to repress apoptosis (Ren et al., 2014). Expression levels of this gene were increased in both iAsT and iAs-rev cells compared to NT cells (Fig. 7A). These gene expression changes correlated positively with the increase in DNA methylation in the gene body of this gene in both iAsT and iAs-rev cells compared to NT cells (Table 1).

Five genes exhibited prominent downregulation after iAs treatment (Fig. 7B). For *CDH12*, expression decreased in iAsT cells and this decrease persisted with iAs-reversal (Fig. 7B). *CDH12* is a type II classical cadherin protein (Shan et al., 2004) and the changes in its expression correlated with gene body hypomethylation, as well as promoter

hypermethylation, in iAsT cells compared to NT cells (Fig. 7B and Table 1). The decrease in expression from iAsT to iAs-rev also correlates with promoter hypermethylation identified in our genome-wide methylation studies. *ARID5B*, which is involved in histone demethylase complexes (Baba et al., 2011), had a decrease in expression in iAsT cells and remained at that level even in iAs-rev cells (Fig. 7B). This is somewhat surprising considering ARID5B has hypomethylation in its promoter region in iAs-rev cells (Table 1). For *DYNC1I2*, a member of the dynein intermediate chain family (Kuta et al., 2010), a decrease in gene expression was observed in iAsT cells compared to NT cells, while iAs removal resulted in upregulation of DYNC1I2 (Fig. 7B), correlating with the promoter hypomethylation observed in the microarray (Table 1). *PRDX1*, a peroxiredoxin family member, showed a decrease in expression during iAs treatment correlating with promoter hypermethylation in iAsT cells (Fig. 7B and Table 1). After removal of iAs, gene expression returned to normal levels (Fig. 7B). Lastly, gene expression at the *EPC1* gene, a polycomb group member (Huang et al., 2014), correlated to the observed methylation changes – decreased gene expression in iAsT cells compared to NT cells with moderate reversal in iAs-rev cells, corresponding with gene body hypomethylation in iAs-rev compared to NT cells. So too, an increase in gene expression in iAs-rev cells compared to iAsT cells corresponded to the observed hypermethylation at the gene body of the *EPC1* gene for iAs-rev v. iAsT (Fig. 7B).

The fact that expression of some genes such as *PPM1L*, *DYNC1I2*, *PRDX1*, and *EPC1* reverted to normal levels in iAs-rev and that those gene expression changes correlate to reversal of DNA methylation patterns suggests the role of epigenetics in this process. However, other changes instigated by iAs treatment were more permanent, such as the gene expression changes seen for *CORO1B*, *PPME1*, *CDH12*, and *ARID5B* and suggest that either these epigenetic factors were not reversed or that other factors together with epigenetics are stabilizing a more permanently changed gene expression state of the gene.

3.9. Global correlation of gene expression pattern with DNA methylation patterns

In order to further understand the biological significance of differential methylation in iAsT and iAs-rev cells, we examined the overlap of genes that were both differentially methylated as well as differentially expressed at the transcript level. For this analysis we reanalyzed our previous dataset (GSE60760) of iAs-mediated differentially expressed genes (Riedmann et al., 2015). To understand the pathways targeted in iAsT, we analyzed the overlap between genes differentially expressed in iAsT cells and those differentially methylated in iAsT cells. There were 270 genes that were both differentially methylated and differentially expressed in cells treated with inorganic arsenic (Supplemental Fig. 5A). For the sake of simplicity, Venn diagram analysis was performed on all genes that were differentially expressed as well as differentially methylated.

We then performed gene ontology (GO) analyses using the Gene Set Enrichment Analysis (GSEA) to identify regulatory pathways affected by both differential methylation and differential expression. Our analyses show that signal transduction pathways and development processes are enriched, indicating that these pathways are targeted by iAs (Table 2). Since we observed that iAsT cells were undergoing EMT, we analyzed the target genes for oncogenic signatures. Our analysis showed that some of the genes with differential

methylation and differential gene expression are involved in abnormal expression of K-RAS (an oncogene) in epithelial cells, particularly lung, breast, and kidney tissue (Supplemental Table 2).

We next asked if these pathways are still targeted in iAs-rev cells. We identified 187 genes that are both differentially methylated and differentially expressed in iAs-rev cells (Supplemental Fig. 5B). These genes represent those whose methylation patterns did not revert to normal levels and were more permanently changed. GO analysis of these genes showed enrichment in biological processes such as development and metabolic processes (Table 3). Investigating the oncogenic signature of these genes also revealed that they are involved in abnormal expression of K-RAS in lung, breast, and kidney epithelial tissue, similarly to iAsT cells (Supplemental Table 3). This could indicate that while some genes are reverting back to normal levels of expression, the genes that do not revert are driving the carcinogenic potential of iAs treatment.

Finally, we investigated those genes that are differentially methylated between iAs-rev cells and iAsT cells. These genes represent the group of genes that are transient and return to a more normalized condition after iAs removal (Supplemental Fig. 5C). GO analysis of these genes revealed enrichment in biological processes such as signal transduction, metabolism, and cell death (Table 4). Their oncogenic signatures again showed dysregulation of K-RAS in epithelial cells in lung, kidney, and breast tissue (Supplemental Table 4). A complete gene ontology listing of these genes with regards to their hyper- and hypomethylation state is found in Supplemental Tables 5–7.

In summary, we show that differential methylation influences differential expression, both during treatment and after the reversal of treatment. While some differential methylation and differential expression changes remained after reversal of treatment, others reversed back to normal conditions. Since the breadth of the impact of methylation is not completely known, we also observed that some methylation patterns which were reversed did not correlate with changes in gene expression. Additionally, it seems that even though some genes are reversed, the cells are still poised in an oncogenic state, as revealed by the oncogenic signatures. However, our data provides a platform enabling the probing of DNA methylation patterns, reversal of those patterns, and the function either in promoting direct gene expression and/or in the possible recruitment of factors that might aid in gene expression. This is especially intriguing as we observed that the K-RAS regulatory process might be specifically targeted by iAs in disease pathogenesis.

4. Discussion

To date, few studies have identified specific gene loci that are differentially methylated in response to chronic iAs exposure. The dose used in our experiments is biologically relevant and mimics the dosage many living in mining regions are exposed to daily (Nordstrom, 2002; IARC, 2004; NTP, 2014). Sadly, in some countries, people are exposed to even higher amounts on a regular basis (Tsuda et al., 1995; Drobná et al., 2013; Koestler et al., 2013). Ours is the first study to distinguish between permanent and reversible DNA methylation changes using data from cells with treatment reversal. The treatment group that experienced

reversal of treatment is also biologically relevant as it imitates the case in which people move away from an area that has chronic low dose arsenic exposure, quit smoking, or otherwise remove themselves from environments where they are experiencing high levels of inorganic arsenic. All of these situations happen frequently and while these people experience a cessation of exposure, the biologic effects may still persist, as shown by this study.

Our studies show that chronic low-dose exposure to iAs leads to global methylation changes (Figs. 2 and 3) as well as differential methylation in gene regulatory regions (Figs. 4–6) and specific genes (Table 1). Differential methylation is concentrated to CGIs (Fig. 4), upstream promoter regions, and gene bodies (Fig. 5). The differential methylation correlates to changes in gene expression which may be a driving factor in the epithelial-to-mesenchymal transition (Figs. 1 and 7). Upon reversal of treatment, some methylation and expression changes revert to normal conditions and others do not (Fig. 7 and Table 1). Ontology analysis of genes targeted in iAs-mediated differential methylation patterns revealed an enrichment of cellular processes, such as cell signaling and development, after initial iAs exposure and enrichment of processes involved in metabolism after iAs withdrawal (Tables 2–4).

Our study is unique in its investigation of biological consequences of removal of iAs exposure. The initial insult of chronic low dose exposure to iAs is clearly detrimental due to its ability to cause cellular transformation and EMT (Riedmann et al., 2015; Rea et al., 2016; Rea et al., 2017). However, the ramifications of iAs exposure do not fully disappear when exposure ends. It appears that while some changes partially revert back to normal conditions after exposure is removed, many changes remain in their abnormal state (Fig. 1). Previous studies showed this partial reversal in morphology, gene expression and protein levels of EMT markers, DNA methylation patterns, and gene expression patterns (Riedmann et al., 2015; Rea et al., 2016; Rea et al., 2017). What we are now showing is methylation and gene expression changes due to withdrawal of iAs exposure. For DNA methylation and its effect on gene expression, we hypothesize that the genes that remain differentially methylated and expressed, such as *CORO1B* and *CDH12*, are driving transformation and EMT, while those that revert back to normal levels of methylation and expression, such as *DYNC1I2* and *EPC1*, are involved in early adaptation to iAs exposure and are less involved in transformation and EMT. Additional studies will be needed to identify specific genes as drivers or passengers. By identifying specific genes that are differentially methylated between iAsT and its withdrawal, we can parse out which genes are still altered after reversal and which revert to a more normal phenotype. We hypothesize that as cells undergo iAs-mediated EMT, hypomethylation may be occurring at oncogenes while hypermethylation may be occurring at tumor suppressors.

We are also intrigued and encouraged by the fact that our previous studies in BEAS-2B cells and our current study in HeLa cells show similar results in EMT markers, DNA methylation patterns, and carcinogenic potential (Riedmann et al., 2015; Rea et al., 2016, 2017). This finding indicates that HeLa cells can be used as an effective model for chronic low-dose iAs-mediated epithelial-to-mesenchymal transition. We witnessed similar changes in cell morphology expression and protein levels of EMT markers in both cell types. Additionally,

we found that DNA methylation instigates changes in gene expression patterns that contribute to EMT for both cell types. Furthermore, HeLa cells and BEAS-2B cells returned similar gene ontology results for pathways and processes that are being targeted in iAs treatment such as cell signaling and neurogenesis (Tables 2–4) (Rea et al., 2017). As would be expected, there were some minor differences between the results we observed in HeLa cells compared to BEAS-2B cells. For example, BEAS-2B cells had slight global hypomethylation while HeLa cells had slight global hypermethylation upon treatment (Rea et al., 2017). Differences could be due to the state of the cells used in the experiments. In our earlier studies, we used non-carcinogenic cells, whereas in this study, HeLa cells are already carcinogenic. Even though one cell line is carcinogenic and the other is not, iAs caused EMT in both and we believe that similar mechanisms are driving EMT in both cell lines. Transformation and carcinogenesis are dynamic processes that rely on several mechanisms, EMT being one of them. It seems that in HeLa cells, iAs treatment pushes EMT even further. It would be interesting to compare the changes seen in BEAS-2B and HeLa to determine which changes are contributing to cellular transformation and which are contributing to EMT.

For the most part, our expression data matched what we would expect based on the methylation present in the gene (Fig. 7). However, a few genes, such as *PPME1*, exhibited expression changes that were opposite of what we would expect due to the methylation data. One explanation is that not every CpG is able to influence gene expression with its methylation status; some CpGs are regulatory and others are not. With so much data, it's possible that not every CpG is regulatory. Some CpGs could be functioning as a location for other transcription factors or proteins to bind that may have functions other than mediating gene expression (Maunakea et al., 2013; Nalabothula et al., 2015). For many of the genes we investigated, there was differential methylation in several regions. In our data set, some genes had antagonistic methylation changes such as hypomethylation at one CpG in the promoter and hypermethylation at another CpG in the same promoter. It's been proposed that methylation may function differently depending on whether it's in an intron or exon (Lev Maor et al., 2015). Further research is needed to answer these questions and to understand the full function of gene body methylation in the context of low dose arsenic exposure. Clearly, we are at the beginning of understanding the full function of DNA methylation. Interestingly, recent studies have linked methylation changes to alterations in alternative splicing patterns (Maunakea et al., 2013; Lev Maor et al., 2015; Yearim et al., 2015). Our own previous studies implicated all of the genes from our gene expression experiment as having alternative splicing changes (Supplemental Table 8).

The vastness of the data we gained from the Infinium MethylationEPIC BeadChip Array underscores the complexity of differential DNA methylation in cells, and therefore the depth of our understanding. For instance, tens of thousands of loci are differentially methylated in response to low dose arsenic exposure and/or reversal of treatment (Fig. 3 and Supplemental Fig. 2); which of them is actually regulatory is the subject of additional study. However, inorganic arsenic is known to cause detrimental effects through mechanisms other than epigenetics, such as reactive oxygen species (Carpenter et al., 2011; Li et al., 2014; Zhang et al., 2015). It is also possible that both mechanisms are working together, enhancing biologic actions to drive the carcinogenic potential of iAs (He et al., 2012; Kang et al., 2012). Further

studies to understand this cooperation would be interesting. In addition to ROS, DNA methylation is also known to interplay with other epigenetic modifications such histone variants and histone post-translational modifications (Chervona et al., 2012; Riedmann et al., 2015; Rea et al., 2016). Because other epigenetic marks are altered in iAs-mediated EMT, it is plausible that they all work collectively. For example, dysregulation of histones H2B and H3 has been implicated in iAs-mediated transformation and EMT (Brocato et al., 2015; Rea et al., 2016). Additionally, alterations in histone post-translational modifications have been shown in iAs-treated conditions including upregulation of the repressive mark H3K27me3 and activation of the mark H3K4me3. It is hypothesized that crosstalk between all of these epigenetic marks – DNA methylation, histone variants, and histone post-translational modifications – control the chromatin landscape present in iAs treated cells. For example, DNA methylation and H3K27me3 are known to be coregulated and both dynamically monitor DNA accessibility and gene expression (Hagarman et al., 2013; de la Calle Mustienes et al., 2015). Therefore, the full implications of iAs exposure cannot fully be appreciated without understanding the crosstalk between epigenetic marks.

In conclusion, this study presents genome-wide changes to DNA methylation levels, as well as changes in gene expression in HeLa cells that were exposed to iAs at chronic low-dose levels, and also in cells that had the arsenic removed. We found that in many cases, the changes seen in cells exposed to iAs returned to near NT levels; these regions may be important in the cellular response to the iAs. However, many genes either do not revert to NT levels, or show an increased change in DNA methylation and gene expression. These genes may be involved in the EMT process that drives the carcinogenic effects with chronic low-dose iAs exposure. Our results provide a platform to develop potential epigenetic therapeutics in iAs-mediated carcinogenesis. Such studies could be extended to other environmental toxicants to enhance the understanding of their impact on the epigenome and gene expression.

Supplementary Material

Refer to Web version on PubMed Central for supplementary material.

Acknowledgments

We would like to thank Hong Quach of the Vincent J. Coates Genomics Sequencing Laboratory at the University of California Berkeley for the Infinium DNA methylation studies. We would also like to thank Donna Gilbreath and Catherine Anthony for editing the manuscript. The GEO accession number for methylation data is GSE60760. This work was supported by NSF grant MCB 1517986 to YFN-M, NIEHS grant R01-ES024478 with diversity supplement 02S1 to YNF-M and NIH T32 grant 165990 to MR, through Markey Cancer Center at University of Kentucky.

Abbreviations

NT	nontreated HeLa cells
iAsT	0.5 μM sodium arsenite treated HeLa cells
iAs-rev	reverse treated cells
EMT	epithelial-to-mesenchymal transition

DMR	Differentially Methylated Region
iAs	inorganic arsenic
DNMTs	DNA methyltransferases
SAM	*S*-adenosyl methionine
CGI	CpG island
AS3MT	arsenic methyltransferase
qRT-PCR	quantitative real time polymerase chain reaction
5mC	5-methylcytosine
5′UTR	5′ untranslated region
3′UTR	3′ untranslated region
TSS	transcription start site
GO	gene ontology
GSEA	Gene Set Enrichment Analysis
H3K4me3	Histone 3 lysine 4 trimethylation
H3K27me3	Histone 3 lysine 27 trimethylation

References

Baba A, Ohtake F, Okuno Y, Yokota K, Okada M, Imai Y, Min N, Meyer CA, Igarashi K, Kanno J, Brown M, Kato S. PKA-dependent regulation of the histone lysine demethylase complex PHF2-ARID5B. Nat. Cell Biol. 2011; 13:669–676.

Bestor TH. The DNA methyltransferases of mammals. Hum. Mol. Genet. 2000; 9:2395–2402. [PubMed: 11005794]

Bird A. DNA methylation patterns and epigenetic memory. Genes Dev. 2002; 16:6–21. [PubMed: 11782440]

Brocato J, Chen D, Liu J, Fang L, Jin C, Costa M. A potential new mechanism of arsenic carcinogenesis: depletion of stem-loop binding protein and increase in polyadenylated canonical histone H3.1 mRNA. Biol. Trace Elem. Res. 2015; 166:72–81. [PubMed: 25893362]

de la Calle Mustienes E, Gómez-Skarmeta JL, Bogdanović O. Genome-wide epigenetic cross-talk between DNA methylation and H3K27me3 in zebrafish embryos. Genomics Data. 2015; 6:7–9. [PubMed: 26697317]

Carpenter RL, Jiang Y, Jing Y, He J, Rojanasakul Y, Liu L-Z, Jiang B-H. Arsenite induces cell transformation by reactive oxygen species, AKT, ERK1/2, and p70S6K1. Biochem. Biophys. Res. Commun. 2011; 414:533–538. [PubMed: 21971544]

Chen H, Li S, Liu J, Diwan BA, Barrett JC, Waalkes MP. Chronic inorganic arsenic exposure induces hepatic global and individual gene hypomethylation: implications for arsenic hepatocarcinogenesis. Carcinogenesis. 2004; 25:1779–1786. [PubMed: 15073043]

Cheng T-F, Choudhuri S, Muldoon-Jacobs K. Epigenetic targets of some toxicologically relevant metals: a review of the literature. J. Appl. Toxicol. 2012; 32:643–653. [PubMed: 22334439]

Chervona Y, Hall MN, Arita A, Wu F, Sun H, Tseng HC, Ali E, Uddin MN, Liu X, Zoroddu MA, Gamble MV, Costa M. Associations between arsenic exposure and global posttranslational histone modifications among adults in Bangladesh. Cancer Epidemiol. Biomark. Prev. 2012; 21:2252–2260.

Collins AR, Ai-guo M, Duthie SJ. The kinetics of repair of oxidative DNA damage (strand breaks and oxidised pyrimidines) in human cells. Mutat. Res. 1995; 336:69–77. [PubMed: 7528897]

Cui X, Wakai T, Shirai Y, Yokoyama N, Hatakeyama K, Hirano S. Arsenic trioxide inhibits DNA methyltransferase and restores methylation-silenced genes in human liver cancer cells. Hum. Pathol. 2006; 37:298–311. [PubMed: 16613325]

Deng B, Zhang S, Miao Y, Zhang Y, Wen F, Guo K. Down-regulation of frizzled-7 expression inhibits migration, invasion, and epithelial–mesenchymal transition of cervical cancer cell lines. Med. Oncol. 2015; 32:1–9.

Drobná Z, Del Razo LM, García-Vargas GG, Sánchez-Peña LC, Barrera-Hernández A, Stýblo M, Loomis D. Environmental exposure to arsenic, AS3MT polymorphism and prevalence of diabetes in Mexico. J. Expo. Environ. Epidemiol. 2013; 23:151–155.

Garcia-Esquinas E, Pollan M, Umans JG, Francesconi KA, Goessler W, Guallar E, Howard B, Farley J, Best LG, Navas-Acien A. Arsenic exposure and cancer mortality in a US-based prospective cohort: the strong heart study. Cancer Epidemiol. Biomark. Prev. 2013; 22:1944–1953.

Goll MG, Bestor TH. Eukaryotic cytosine methyltransferases. Annu. Rev. Biochem. 2005; 74:481–514. [PubMed: 15952895]

Hagarman JA, Motley MP, Kristjansdottir K, Soloway PD. Coordinate regulation of DNA methylation and H3K27me3 in mouse embryonic stem cells. PLoS One. 2013; 8:e53880. [PubMed: 23326524]

Harris GK, Shi X. Signaling by carcinogenic metals and metal-induced reactive oxygen species. Mutat. Res. 2003; 533:183–200. [PubMed: 14643420]

He J, Xu Q, Jing Y, Agani F, Qian X, Carpenter R, Li Q, Wang X-R, Peiper SS, Lu Z, Liu L-Z, Jiang B-H. Reactive oxygen species regulate ERBB2 and ERBB3 expression via miR-199a/125b and DNA methylation. EMBO Rep. 2012; 13:1116–1122. [PubMed: 23146892]

Hopenhayn-Rich C, Biggs ML, Smith AH. Lung and kidney cancer mortality associated with arsenic in drinking water in Córdoba, Argentina. Int. J. Epidemiol. 1998; 27:561–569. [PubMed: 9758107]

Huang C, Ma W-Y, Li J, Goranson A, Dong Z. Requirement of Erk, but not JNK, for arsenite-induced cell transformation. J. Biol. Chem. 1999; 274:14595–14601. [PubMed: 10329651]

Huang C, Ke Q, Costa M, Shi X. Molecular mechanisms of arsenic carcinogenesis. Mol. Cell. Biochem. 2004; 255:57–66. [PubMed: 14971646]

Huang X, Spencer GJ, Lynch JT, Ciceri F, Somerville TDD, Somervaille TCP. Enhancers of Polycomb EPC1 and EPC2 sustain the oncogenic potential of MLL leukemia stem cells. Leukemia. 2014; 28:1081–1091. [PubMed: 24166297]

IARC. Some drinking-water disinfectants and contaminants, including arsenic. IARC Monogr. Eval. Carcinog. Risks Hum. 2004; 84:39–267.

Jjingo D, Conley AB, Yi SV, Lunyak VV, Jordan IK. On the presence and role of human gene-body DNA methylation. Oncotarget. 2012; 3:462–474. [PubMed: 22577155]

Johnson N, Shelton BJ, Hopenhayn C, Tucker TT, Unrine JM, Huang B, Christian WJ, Zhang Z, Shi X, Li L. Concentrations of arsenic, chromium, and nickel in toenail samples from Appalachian Kentucky residents. J. Environ. Pathol. Toxicol. Oncol. 2011; 30:213–223. [PubMed: 22126614]

Kang KA, Zhang R, Kim GY, Bae SC, Hyun JW. Epigenetic changes induced by oxidative stress in colorectal cancer cells: methylation of tumor suppressor RUNX3. Tumor Biol. 2012; 33:403–412.

Klein CB, Leszczynska J, Hickey C, Rossman TG. Further evidence against a direct genotoxic mode of action for arsenic-induced cancer. Toxicol. Appl. Pharmacol. 2007; 222:289–297. [PubMed: 17316729]

Koestler DC, Avissar-Whiting M, Houseman EA, Karagas MR, Marsit CJ. Differential DNA methylation in umbilical cord blood of infants exposed to low levels of arsenic in utero. Environ. Health Perspect. 2013; 121:971–977. [PubMed: 23757598]

Kuta A, Deng W, Morsi El-Kadi A, Banks GT, Hafezparast M, Pfister KK, Fisher EMC. Mouse cytoplasmic dynein intermediate chains: identification of new isoforms, alternative splicing and tissue distribution of transcripts. PLoS One. 2010; 5:e11682. [PubMed: 20657784]

Lev Maor G, Yearim A, Ast G. The alternative role of DNA methylation in splicing regulation. Trends Genet. 2015; 31:274–280. [PubMed: 25837375]

Li J, Chen P, Sinogeeva N, Gorospe M, Wersto RP, Chrest FJ, Barnes J, Liu Y. Arsenic trioxide promotes histone H3 phosphoacetylation at the chromatin of CAS-PASE-10 in acute promyelocytic leukemia cells. J. Biol. Chem. 2002; 277:49504–49510. [PubMed: 12388546]

Li L, Wang J, Ye RD, Shi G, Jin H, Tang X, Yi J. PML/RARα fusion protein mediates the unique sensitivity to arsenic cytotoxicity in acute promyelocytic leukemia cells: mechanisms involve the impairment of cAMP signaling and the aberrant regulation of NADPH oxidase. J. Cell. Physiol. 2008; 217:486–493. [PubMed: 18636556]

Li L, Qiu P, Chen B, Lu Y, Wu K, Thakur C, Chang Q, Sun J, Chen F. Reactive oxygen species contribute to arsenic-induced EZH2 phosphorylation in human bronchial epithelial cells and lung cancer cells. Toxicol. Appl. Pharmacol. 2014; 276:165–170. [PubMed: 24582688]

Li H, Wang Y, Xu W, Dong L, Guo Y, Bi K, Zhu C. Arsenic trioxide inhibits DNA methyltransferase and restores TMS1 gene expression in K562 cells. Acta Haematol. 2015a; 133:18–25. [PubMed: 24993472]

Li X-W, Tuergan M, Abulizi G. Expression of MAPK1 in cervical cancer and effect of MAPK1 gene silencing on epithelial-mesenchymal transition, invasion and metastasis. Asian Pac J Trop Med. 2015b; 8:937–943. [PubMed: 26614994]

Lizio M, Harshbarger J, Shimoji H, Severin J, Kasukawa T, Sahin S, Abugessaisa I, Fukuda S, Hori F, Ishikawa-Kato S, Mungall CJ, Arner E, Baillie JK, Bertin N, Bono H, de Hoon M, Diehl AD, Dimont E, Freeman TC, Fujieda K, Hide W, Kaliyaperumal R, Katayama T, Lassmann T, Meehan TF, Nishikata K, Ono H, Rehli M, Sandelin A, Schultes EA, 't Hoen PAC, Tatum Z, Thompson M, Toyoda T, Wright DW, Daub CO, Itoh M, Carninci P, Hayashizaki Y, Forrest ARR, Kawaji H. The, F.c. Gateways to the FANTOM5 promoter level mammalian expression atlas. Genome Biol. 2015; 16:22. [PubMed: 25723102]

Maunakea AK, Chepelev I, Cui K, Zhao K. Intragenic DNA methylation modulates alternative splicing by recruiting MeCP2 to promote exon recognition. Cell Res. 2013; 23:1256–1269. [PubMed: 23938295]

Miao Z, Wu L, Lu M, Meng X, Gao B, Qiao X, Zhang W, Xue D. Analysis of the transcriptional regulation of cancer-related genes by aberrant DNA methylation of the cis-regulation sites in the promoter region during hepatocyte carcinogenesis caused by arsenic. Oncotarget. 2015 Aug 28; 6(25):21493–506. [PubMed: 26046465]

Nalabothula N, Al-jumaily T, Eteleeb AM, Flight RM, Xiaorong S, Moseley H, Rouchka EC, Fondufe-Mittendorf YN. Genome-wide profiling of PARP1 reveals an interplay with gene regulatory regions and DNA methylation. PLoS One. 2015; 10:e0135410. [PubMed: 26305327]

Nordstrom DK. Public health. Worldwide occurrences of arsenic in ground water. Science. 2002; 296:2143–2145. [PubMed: 12077387]

NTP. Report on Carcinogens. Thirteenth. Department of Health and Human Services, Public Health Service; Research Triangle Park, NC: U.S: 2014.

Perini G, Diolaiti D, Porro A, Della Valle G. In vivo transcriptional regulation of N-Myc target genes is controlled by E-box methylation. Proc. Natl. Acad. Sci. U. S. A. 2005; 102:12117–12122. [PubMed: 16093321]

Puustinen P, Junttila MR, Vanhatupa S, Sablina AA, Hector ME, Teittinen K, Raheem O, Ketola K, Lin S, Kast J, Haapasalo H, Hahn WC, Westermarck J. PME-1 protects ERK pathway activity from protein phosphatase 2A-mediated inactivation in human malignant glioma. Cancer Res. 2009; 69:2870–2877. [PubMed: 19293187]

Rea M, Jiang T, Eleazer R, Eckstein M, Marshall AG, Fondufe-Mittendorf YN. Quantitative mass spectrometry reveals changes in histone H2B variants as cells undergo inorganic arsenic-mediated cellular transformation. Mol. Cell. Proteomics. 2016 Jul; 15(7):2411–22. http://dx.doi.org/10.1074/mcp.M116.058412. [PubMed: 27169413]

Rea M, Eckstein M, Eleazer R, Smith C, Fondufe-Mittendorf YN. Genome-wide DNA methylation reprogramming in response to inorganic arsenic links inhibition of CTCF binding, DNMT expression and cellular transformation. Sci. Report. 2017 Feb 2.7:41474. http://dx.doi.org/10.1038/srep41474.

Ren S, Lu G, Ota A, Zhou ZH, Vondriska TM, Lane TF, Wang Y. IRE1 phosphatase PP2Ce regulates adaptive ER stress response in the postpartum mammary gland. PLoS One. 2014; 9:e111606. [PubMed: 25369058]

Riedmann C, Ma Y, Melikishvili M, Godfrey S, Zhang Z, Chen K, Rouchka EC, Fondufe-Mittendorf YN. Inorganic arsenic-induced cellular transformation is coupled with genome wide changes in chromatin structure, transcriptome and splicing patterns. BMC Genomics. 2015; 16:212. [PubMed: 25879800]

Robertson KD. DNA methylation and human disease. Nat. Rev. Genet. 2005; 6:597–610. [PubMed: 16136652]

Rossman TG. Mechanism of arsenic carcinogenesis: an integrated approach. Mutat. Res. 2003; 533:37–65. [PubMed: 14643412]

Rossman TG, Uddin AN, Burns FJ, Bosland MC. Arsenite is a cocarcinogen with solar ultraviolet radiation for mouse skin: an animal model for arsenic carcinogenesis. Toxicol. Appl. Pharmacol. 2001; 176:64–71. [PubMed: 11578149]

Salnikow K, Zhitkovich A. Genetic and epigenetic mechanisms in metal carcinogenesis and cocarcinogenesis: nickel, arsenic and chromium. Chem. Res. Toxicol. 2008; 21:28–44. [PubMed: 17970581]

Shan W, Yagita Y, Wang Z, Koch A, Svenningsen AF, Gruzglin E, Pedraza L, Colman DR. The minimal essential unit for cadherin-mediated intercellular adhesion comprises extracellular domains 1 and 2. J. Biol. Chem. 2004; 279:55914–55923. [PubMed: 15485826]

Siggens L, Ekwall K. Epigenetics, chromatin and genome organization: recent advances from the ENCODE project. J. Intern. Med. 2014; 276:201–214. [PubMed: 24605849]

States JC, Srivastava S, Chen Y, Barchowsky A. Arsenic and cardiovascular disease. Toxicol. Sci. 2009; 107:312–323. [PubMed: 19015167]

Suzuki MM, Bird A. DNA methylation landscapes: provocative insights from epigenomics. Nat. Rev. Genet. 2008; 9:465–476. [PubMed: 18463664]

Tapio S, Grosche B. Arsenic in the aetiology of cancer. Mutat. Res. 2006; 612:215–246. [PubMed: 16574468]

The, E.P.C. An integrated encyclopedia of DNA elements in the human genome. Nature. 2012; 489:57–74. [PubMed: 22955616]

Tseng WP, Chu HM, How SW, Fong JM, Lin CS, Yeh S. Prevalence of skin cancer in an endemic area of chronic arsenicism in Taiwan. J. Natl. Cancer Inst. 1968; 40:453–463. [PubMed: 5644201]

Tsuda T, Babazono A, Yamamoto E, Kurumatani N, Mino Y, Ogawa T, Kishi Y, Aoyama H. Ingested arsenic and internal cancer: a historical cohort study followed for 33 years. Am. J. Epidemiol. 1995; 141:198–209. [PubMed: 7840093]

Williams, HC., Martín, AS., Adamo, CM., Seidel-Rogol, B., Pounkova, L., Datla, SR., Lassègue, B., Bear, JE., Griendling, K. Role of coronin 1B in PDGF-induced migration of vascular smooth muscle cells; Circ. Res. 2012. p. 111http://dx.doi.org/10.1161/CIRCRESAHA.1111.255745

Xiao W, Zhou S, Xu H, Li H, He G, Liu Y, Qi Y. Nogo-B promotes the epithelial-mesenchymal transition in HeLa cervical cancer cells via Fibulin-5. Oncol. Rep. 2013; 29:109–116. [PubMed: 23042479]

Yang X, Han H, De Carvalho DD, Lay FD, Jones PA, Liang G. Gene body methylation can alter gene expression and is a therapeutic target in cancer. Cancer Cell. 2014; 26:577–590. [PubMed: 25263941]

Yearim A, Gelfman S, Shayevitch R, Melcer S, Glaich O, Mallm JP, Nissim-Rafinia M, Cohen AH, Rippe K, Meshorer E. Ast, G. HP1 is involved in regulating the global impact of DNA methylation on alternative splicing. Cell Rep. 2015; 10:1122–1134. [PubMed: 25704815]

Zhang Z, Pratheeshkumar P, Son Y-O, Kim D, Shi X. Role of reactive oxygen species in arsenic-induced transformation of human lung bronchial epithelial (BEAS-2B) cells. Biochem. Biophys. Res. Commun. 2015; 456:643–648. [PubMed: 25499816]

Zhou X, Sun H, Ellen TP, Chen H, Costa M. Arsenite alters global histone H3 methylation. Carcinogenesis. 2008; 29:1831–1836. [PubMed: 18321869]

Zhou X, Sun X, Cooper KL, Wang F, Liu KJ, Hudson LG. Arsenite interacts selectively with zinc finger proteins containing C3H1 or C4 motifs. J. Biol. Chem. 2011; 286:22855–22863. [PubMed: 21550982]

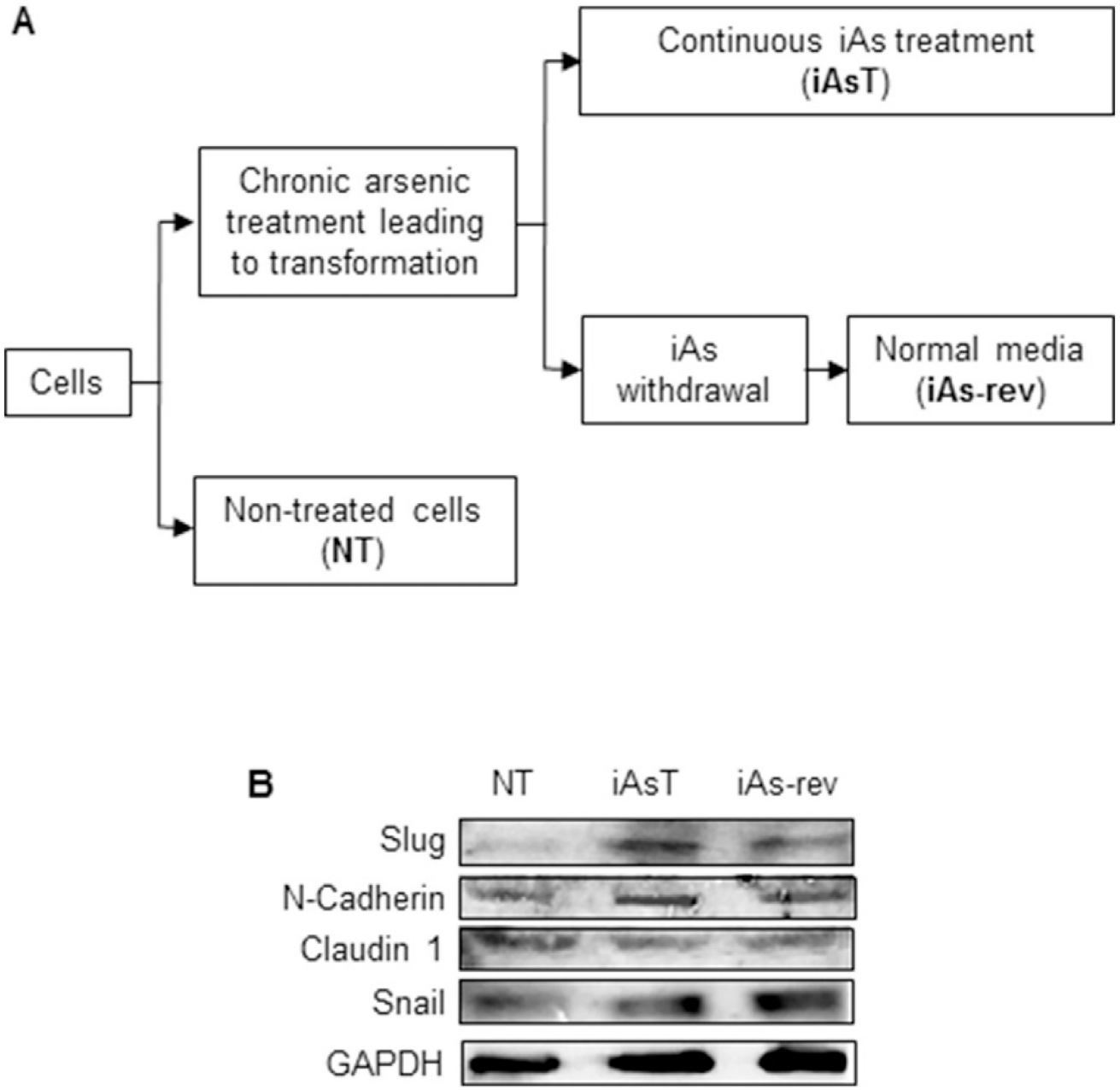

Fig. 1.

Chronic low-dose exposure to iAs and subsequent reversal causes cells to undergo EMT. (A). Diagram of experimental design. HeLa cells were treated with 0.5 μM sodium arsenite (iAsT) while some were mock treated with dIH_2O (NT). After 36 days of iAs treatment, sodium arsenite was removed from growth media for some treated cells and replaced with dIH_2O (iAs-rev); (B). western blot analysis of EMT markers show HeLa cells undergoing iAs-induced EMT. Claudin-1 decreased with treatment, and remained decreased in the iAs-rev condition. Some markers, like Snail, increased in the iAsT, but did not return towards NT levels in iAs-rev cells while *N*-cadherin and Slug increased in iAsT and returned towards NT levels.

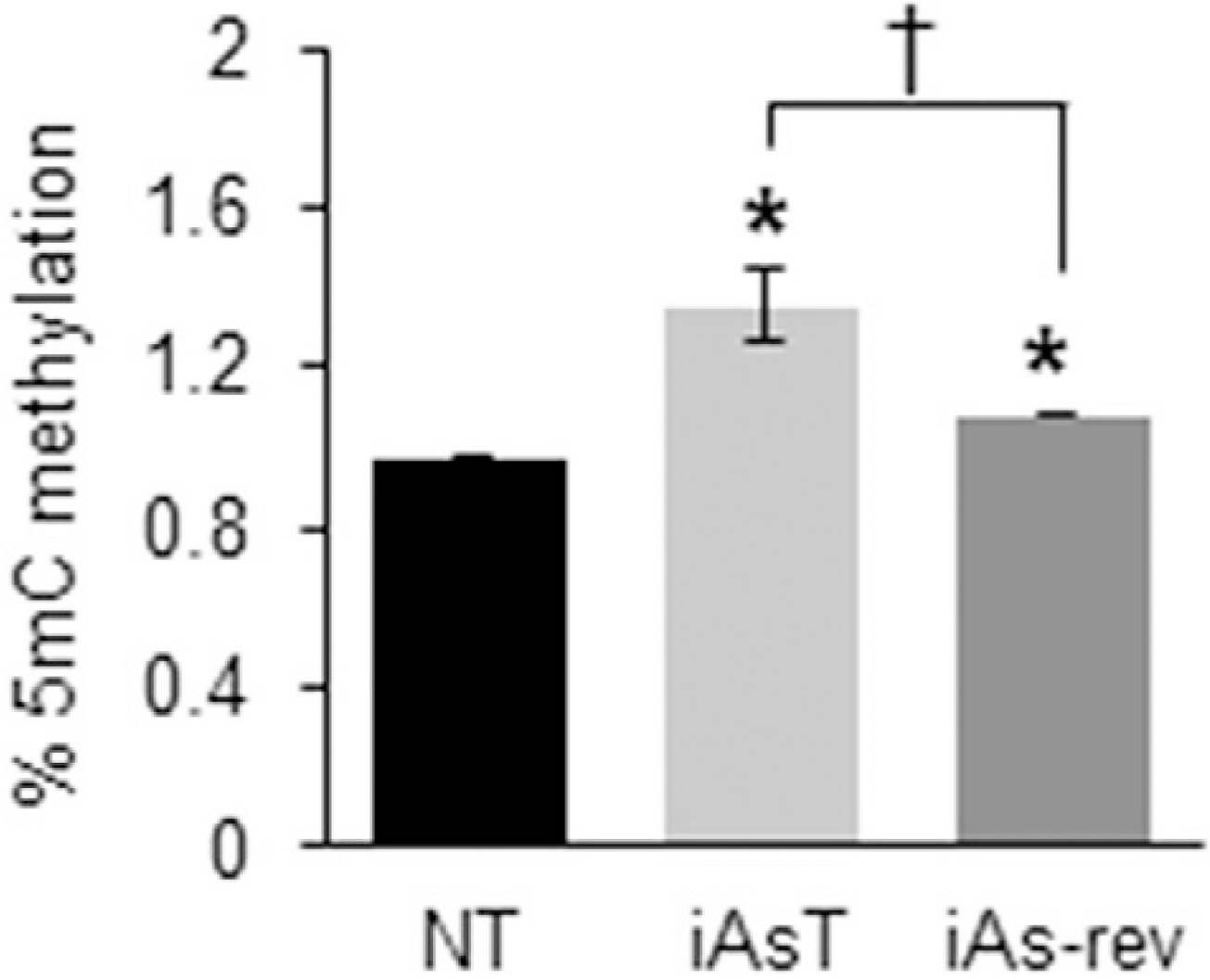

Fig. 2.

Global DNA methylation levels are increased with 0.5 μM arsenite exposure. Results from the 5mC-ELISA show that 0.5 μM sodium arsenite exposure significantly increased global DNA methylation levels in HeLa cells. iAsT cells that had exposure removed (iAs-rev) showed a significant decrease from the iAsT DNA methylation levels; however, these are still significantly increased from NT levels. ELISA was performed in triplicate and error bars reflect the SEM of these replicates. Students *t*-test was performed for significance ($p < 0.05$); * denotes difference from NT † denotes difference from iAsT to iAs-rev.

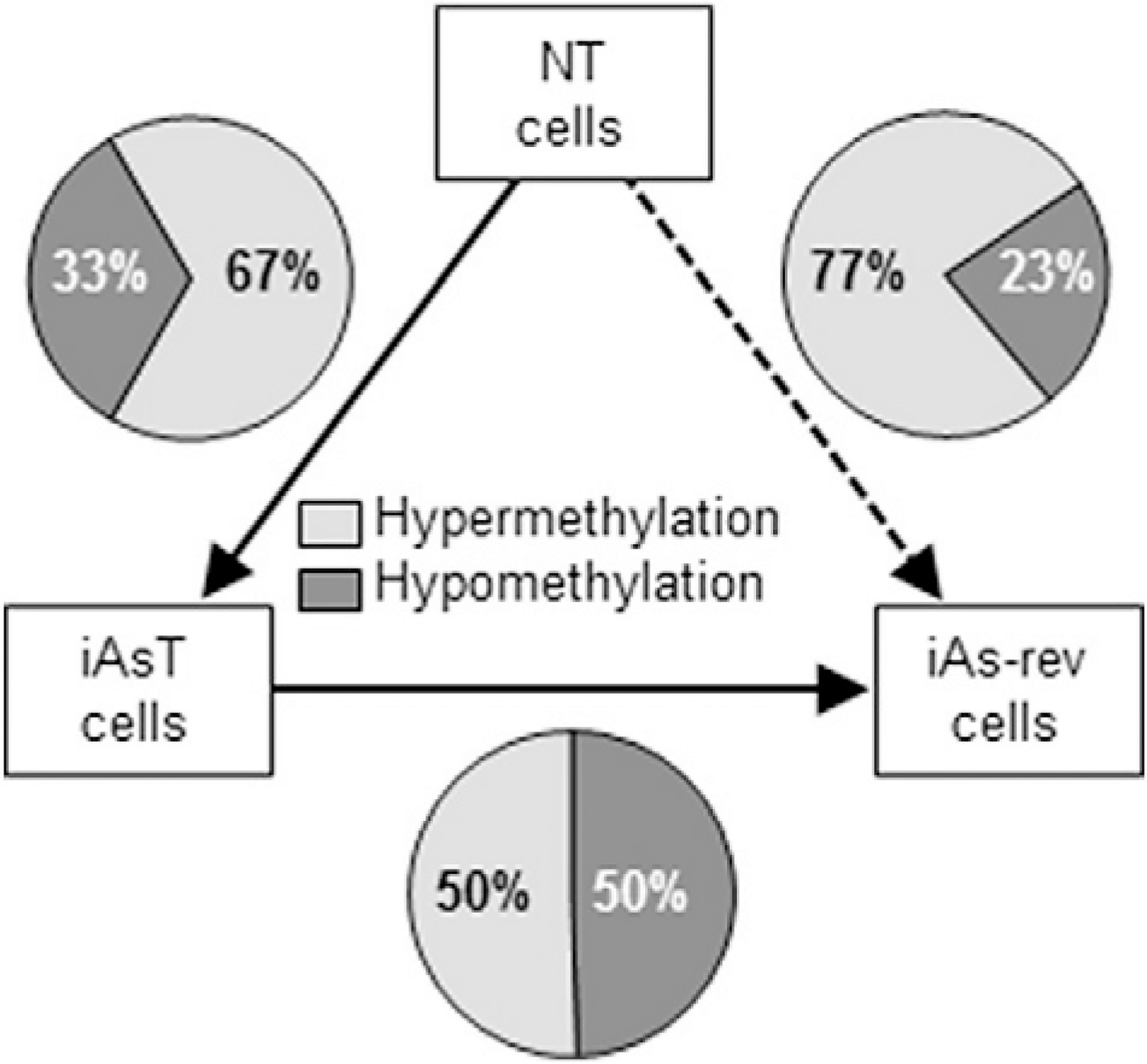

Fig. 3.

Methylation EPIC BeadChip Assay reveals global DNA methylation changes between NT, iAsT, and iAs-rev. Comparison of loci from NT v. iAsT shows that 67% of loci on the chip are hypermethylated in iAsT, while only 33% are hypomethylated. Comparison of methylation loci between NT and iAs-rev shows that 77% of loci are hypermethylated in iAs-rev while only 23% are hypomethylated. Comparison of iAsT and iAs-rev reveals that the loci are approximately equal for hyper- and hypomethylation, suggesting that when iAs is removed many loci return towards NT levels.

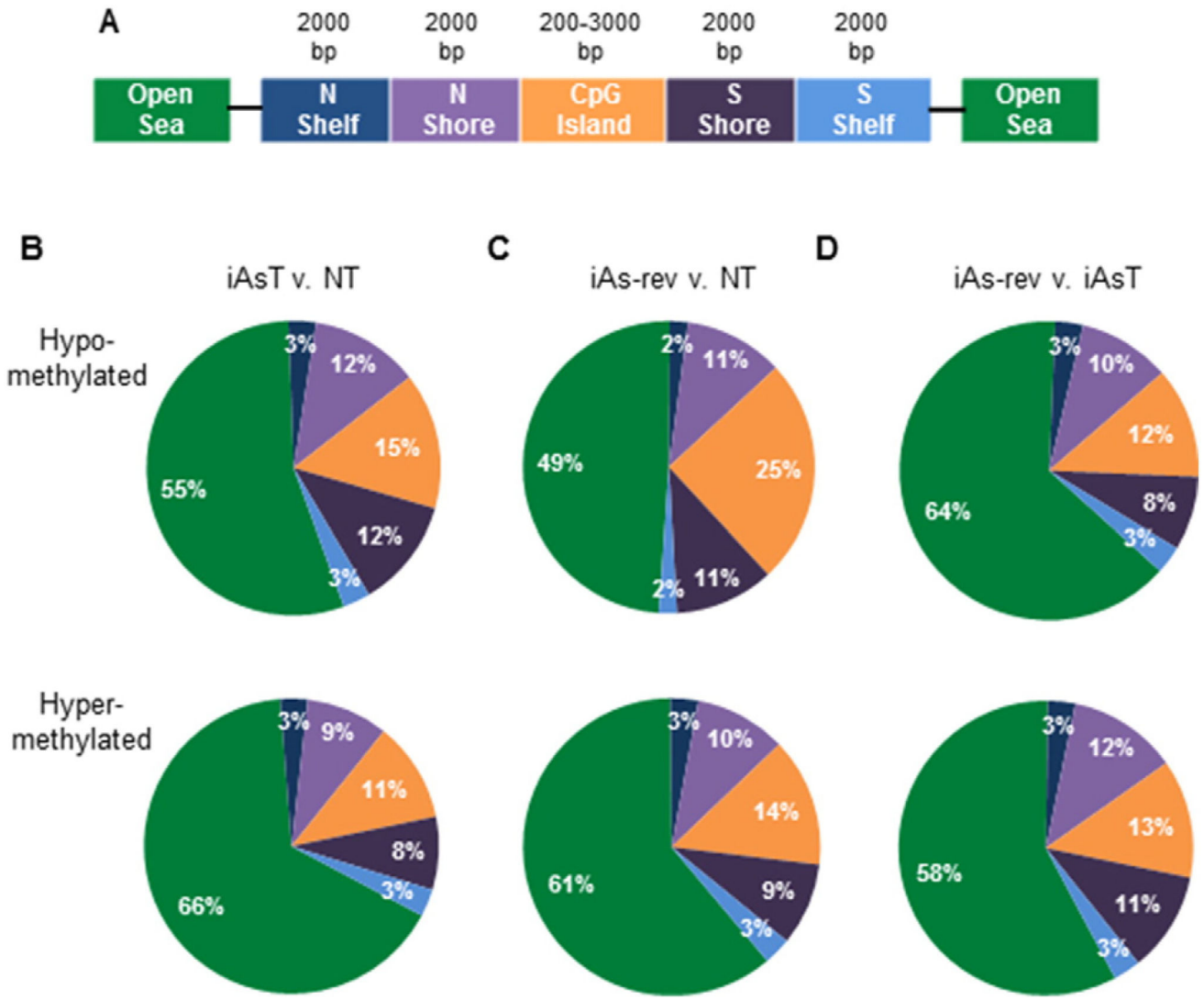

Fig. 4.

DNA methylation patterns show changes both within CGIs and outside of CGIs during iAs-mediated EMT. (A). Diagram showing the relationship of CGIs and neighboring regions. CGI is defined as >50% CG content in at least a 200 base pair region. The north shore is 0–2000 bp upstream of the CGI and north shelf is 2001–4000 bp upstream of the CGI. The south shore is 0–2000 bp downstream of the CGI and the south shelf is 2001–4000 bp downstream of the CGI. Open sea regions are >4000 bp outside of the CGI. (B). Regional methylation changes between iAsT v. NT (C). Regional methylation changes between iAs-rev v. NT (D). Regional methylation changes between iAs-rev v. iAsT. Levels of methylation in shelves and shores stay relatively unchanged between groups and hyper- or hypomethylation. Prominent methylation changes occur at the CGIs and out in the open seas.

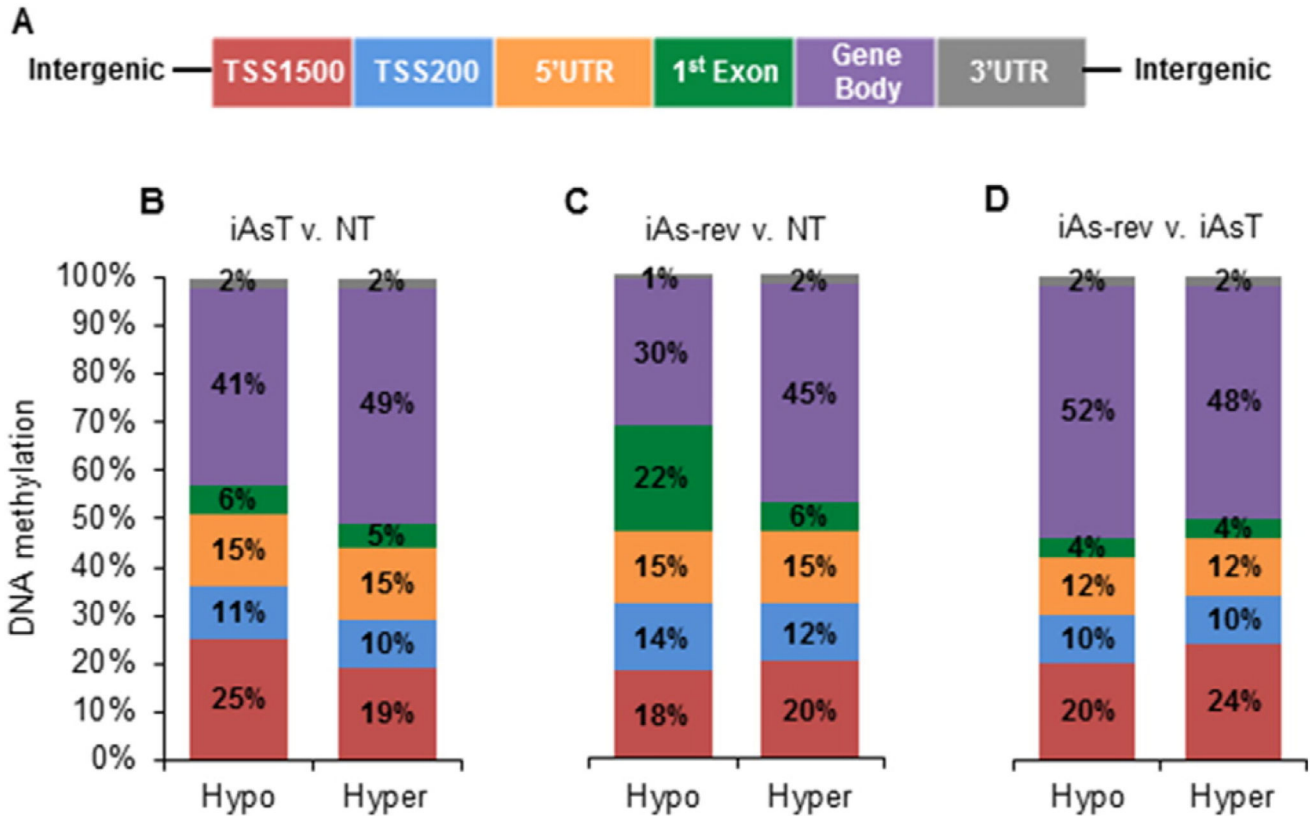

Fig. 5.

DNA methylation patterns within gene regulatory regions reveal large changes within gene bodies, at the 1st exon, and 200–1500 bp upstream of start of transcription. (A). Diagram mapping gene regulatory regions. TSS1500 is 200–1500 bp upstream of transcription start site (TSS), TSS200 is 1–200 bp upstream of TSS, 5′UTR is the 5′ untranslated region, 1st exon is the first translated region, gene body includes all other exons and all introns, and 3′UTR is the 3′ untranslated region where translation ends. Outside of the TSS1500 and 3′UTR is considered intergenic. (B). Gene regulatory methylation differences between iAsT and NT. (C). Gene regulatory methylation differences between iAs-rev and NT. (D). Gene regulatory methylation differences between iAs-rev and iAsT. Methylation within gene regulatory regions is generally stable throughout the treatment groups. Gene body and TSS1500 methylation shows the most variation between hyper- and hypomethylated DMRs.

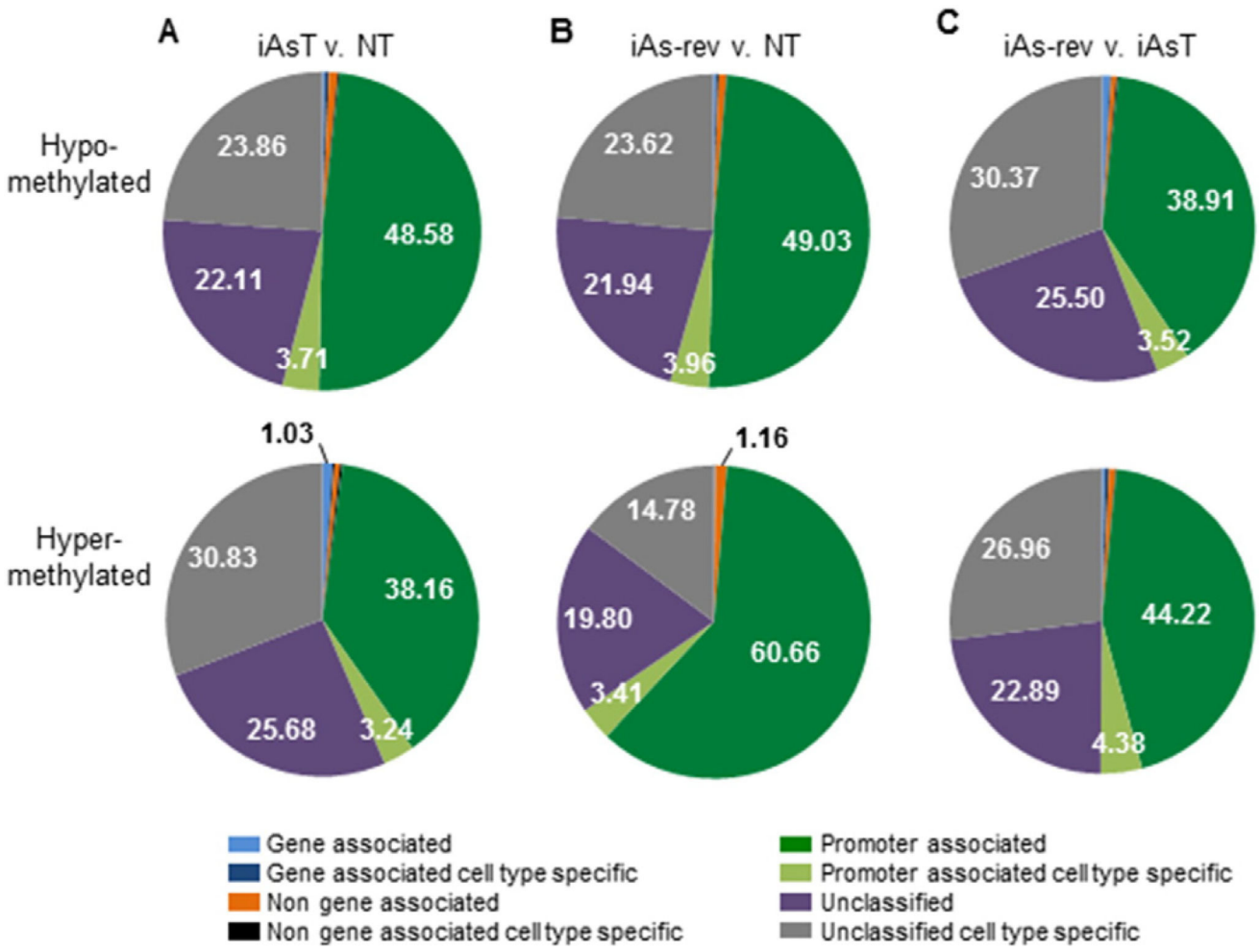

Fig. 6.

DNA methylation level changes at promoter associated regions reveal large changes within the promoter and unclassified regions. Comparison of DMRs within different promoter types. (A). Regional promoter-associated methylation differences between iAsT and NT. (B). Regional promoter-associated methylation differences between iAs-rev and NT. (C). Regional promoter-associated methylation differences between iAs-rev and iAsT. Promoter methylation changes are most apparent at promoter associated (dark green) and unclassified regions (purple), which suggests that iAs targets distinct promoters and regions in methylation changes.

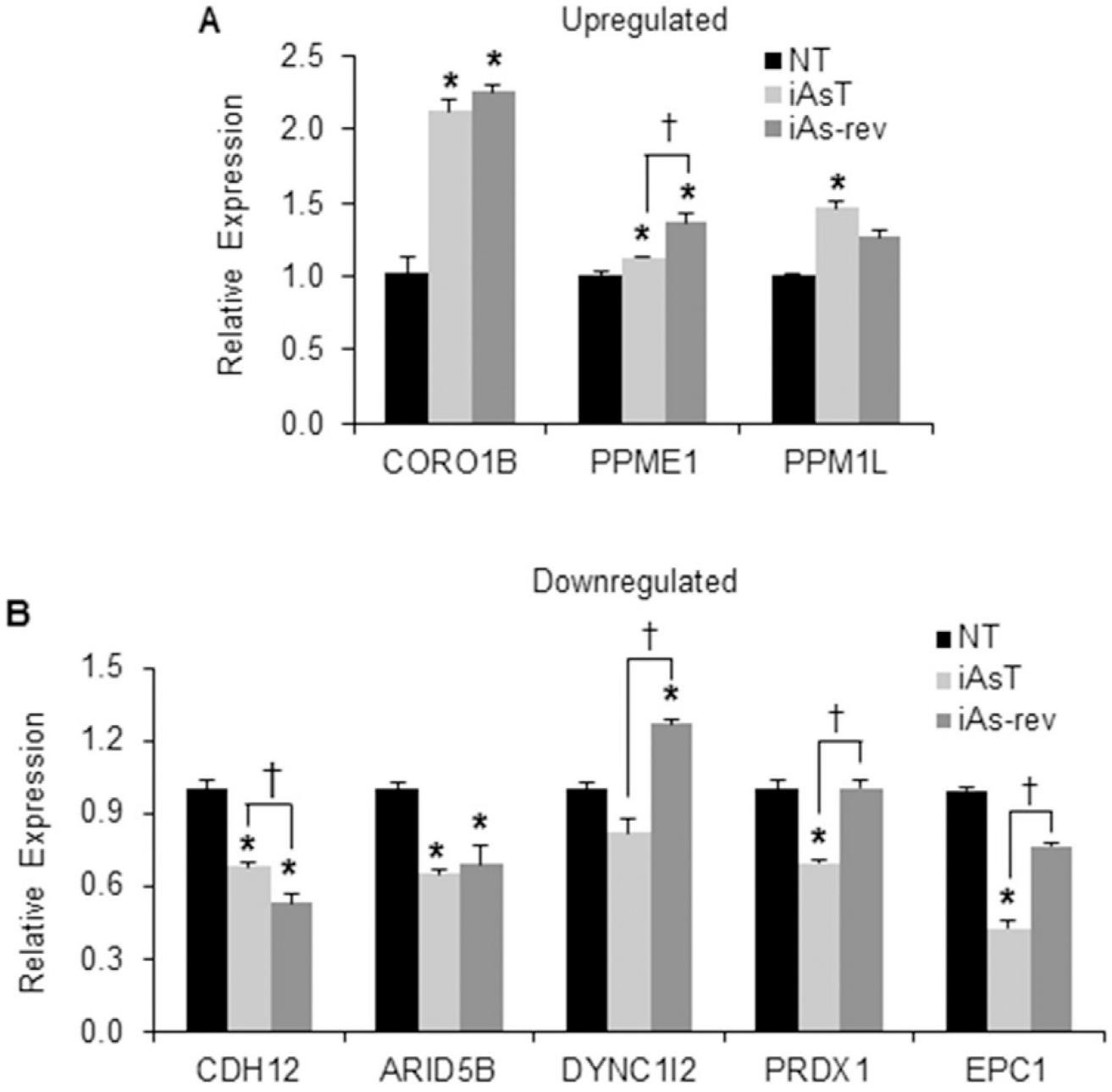

Fig. 7.

Correlation of differential methylation and gene expression. (A). Three genes were upregulated with iAs treatment. *CORO1B* and *PPME1* both increased in expression with iAsT and a further increase was observed in iAs-rev. *PPM1L* increased in iAsT, but shifted towards NT levels with iAs-rev. (B). Seven genes were downregulated with iAs treatment. *CDH12* and *ARID5B* decreased expression levels with iAsT as well as with iAs-rev. *DYNC12, PRDX1* and *EPC1* all decreased expression levels with iAsT, but with iAs-rev the expression levels increased closer to or even above NT levels. qRT-PCR reactions were performed in triplicate. * indicates a significant change when iAsT or iAs-rev is compared to NT and † indicates a significant change between iAsT and iAs-rev with p-value < 0.05.

Error bars are from triplicate experiments and represent SEM.

Table 1

Expected methylation patterns for genes investigated for gene expression changes.

	Gene Region	**iAsT Methylation**	**iAsT Expected Expression**	**iAs-rev Methylation**	**iAsT Expected Expression**
CORO1B	*Promoter*	Hypomethylation	Upregulated	NA	NA
PPME1	*Promoter*	Hypermethylation	Downregulated	NA	NA
PPM1L	*Gene Body*	Hypermethylation	Upregulated	Hypermethylation	Upregulated
CDH12	*Gene Body*	Hypomethylation	Downregulated	NA	NA
ARID5B	*Promoter*	NA	NA	Hypomethylation	Upregulated
DYNC1I2	*Promoter*	NA	NA	Hypomethylation	Upregulated
PRDX1	*Promoter*	Hypermethylation	Downregulated	Hypermethylation	Downregulated
EPCI	*Gene Body*	NA	NA	Hypomethylation	Downregulated

Methylation patterns identified by the Infinium BeadChip Microarray for each gene that was investigated for gene expression changes by qRT-PCR; the expected gene expression patterns based on methylation are presented. Shaded cells indicate that the expected expression was validated by our qRT-PCR results.

Toxicol Appl Pharmacol. Author manuscript; available in PMC 2017 December 30.

Table 2

Gene ontology of differentially methylated and differentially expressed genes (iAsT v. NT).

GO term	Number of genes	p-Value
Intracellular signal transduction	36	3.05E−13
Intrinsic component of plasma membrane	36	1.22E−12
Receptor binding	32	2.93E−11
Cell development	31	5.74E−11
Tissue development	32	5.97E−11
Movement of cell or subcellular component	29	8.81E−11
Regulation of cell death	30	5.52E−10
Response to endogenous stimulus	29	1.67E−09
Negative regulation of response to stimulus	28	1.74E−09
Protein phosphorylation	23	2.43E−09

Gene ontology terms of differentially methylated and differentially expressed genes comparing iAsT to NT (270 total genes).

Table 3

Gene ontology of differentially methylated and differentially expressed genes (iAs-rev v. NT).

GO term	Number of genes	p-Value
Intrinsic component of plasma membrane	32	3.90E−14
Cell development	23	7.07E−09
Response to oxygen containing compound	22	1.92E−08
Small molecule metabolic process	25	1.96E−08
Response to nitrogen compound	17	4.21E−08
Tissue development	22	9.99E−08
Neuron part	20	1.01E−07
Cell junction	19	1.11E−07
Cytoskeleton	25	1.52E−07
Response to endogenous stimulus	21	2.02E−07

Gene ontology terms of differentially methylated and differentially expressed genes comparing iAs-rev to NT (187 total genes).

Table 4

Gene ontology of differentially methylated and differentially expressed genes (iAs-rev v. iAsT).

GO term	Number of genes	p-value
Intrinsic component of plasma membrane	46	5.76E−17
Receptor binding	38	4.46E−13
Intracellular signal transduction	39	6.68E−13
Regulation of cell death	36	8.35E−12
Phosphate containing compound metabolic process	42	1.18E−11
Negative regulation of cell death	27	2.35E-11
Response to endogenous stimulus	35	2.39E−11
Response to oxygen containing compound	34	2.79E−11
Biological adhesion	29	4.15E−11
Neurogenesis	34	4.16E−11

Gene ontology terms of differentially methylated and differentially expressed genes comparing iAs-rev to iAsT (322 total genes).